

The natural emissions model (NEMO): Description, application and model evaluation

Natalia Liora^{*}, Konstantinos Markakis¹, Anastasia Poupkou, Theodore M. Giannaros², Dimitrios Melas

Aristotle University of Thessaloniki, Department of Physics, Laboratory of Atmospheric Physics, 54124 Thessaloniki, Greece



HIGHLIGHTS

- A new natural emissions model for Europe integrates well-documented methodologies.
- Very good model performance in comparison with existing uncertainties.
- Windblown dust emissions are the highest in summertime in Southern Europe.
- Sea salt emissions are the highest in Atlantic Ocean in autumn.
- During summer sea salt emissions are the highest in Mediterranean Sea.

ARTICLE INFO

Article history:

Received 18 August 2015

Received in revised form

6 October 2015

Accepted 7 October 2015

Available online 22 October 2015

Keywords:

Natural emissions model

Particulate matter

Model evaluation

Europe

ABSTRACT

The aim of this study is the application and evaluation of a new computer model used for the quantification of emissions coming from natural sources. The Natural Emissions Model (NEMO) is driven by the meteorological data of the mesoscale numerical Weather Research and Forecasting (WRF) model and it estimates particulate matter (PM) emissions from windblown dust, sea salt aerosols (SSA) and primary biological aerosol particles (PBAPs). It also includes emissions from Biogenic Volatile Organic Compounds (BVOCs) from vegetation; however, this study focuses only on particle emissions. An application and evaluation of NEMO at European scale are presented. NEMO and the modelling system consisted of WRF model and the Comprehensive Air Quality Model with extensions (CAMx) were applied in a 30 km European domain for the year 2009. The computed domain-wide annual PM10 emissions from windblown dust, sea salt and PBAPs were 0.57 Tg, 20 Tg and 0.12 Tg, respectively. PM2.5 represented 6% and 33% of emitted windblown dust and sea salt, respectively. Natural emissions are characterized by high geographical and seasonal variations; windblown dust emissions were the highest during summer in the southern Europe and SSA production was the highest in Atlantic Ocean during the cold season while in Mediterranean Sea the highest SSA emissions were found over the Aegean Sea during summer. Modelled concentrations were compared with surface station measurements and showed that the model captured fairly well the contribution of the natural sources to PM levels over Europe. Dust concentrations correlated better when dust transport events from Sahara desert were absent while the simulation of sea salt episodes led to an improvement of model performance during the cold season.

© 2015 Elsevier Ltd. All rights reserved.

1. Introduction

Emissions of natural environments stem from numerous sources such as vegetation, biomass burning, soils, water bodies, animals, wetlands, volcanoes, lightning, windblown dust (WD) and biological aerosols (NATAIR, 2007; Poupkou et al., 2014). Particulate matter (PM) emissions from natural sources play a significant role in a variety of atmospheric processes that influence climate, air quality and therefore human health. Previous studies emphasized

* Corresponding author.

E-mail address: lioranat@auth.gr (N. Liora).

¹ Laboratoire de Meteorologie Dynamique, IPSL Laboratoire CEA/CNRS/UVSQ, Ecole Polytechnique, 91128 Palaiseau CEDEX, France.

² National Observatory of Athens, Institute for Environmental Research and Sustainable Development, Vas. Pavlou & I. Metaxa, 15 236, Athens, Greece.

on the impact of mineral dust on European air quality (Schaap et al., 2009; Vautard et al., 2005) while others have shown a cumulative effect with particles of anthropogenic origin that increases the aerosol burden in urban centres that are close to the large African dust reservoirs (Athanasopoulou et al., 2010). Dust particles also affect human health (Karanasiou et al., 2012). Sea salt aerosols (SSA) are abundant in the remote marine surface air and therefore they have a significant impact on continental air masses (NATAIR, 2007). SSA can modify the distribution of inorganic aerosols (Im et al., 2012) while in coastal areas they enhance PM levels modifying the chemical composition of PM (Athanasopoulou et al., 2008). Chronic health impacts (allergies, asthma and other diseases) of primary biological aerosol particles (PBAPs) have also been documented (Dillon et al., 1999). Finally, there are plentiful studies pointing to the significance of Biogenic Volatile Organic Compounds (BVOCs) to the formation of tropospheric ozone (Curci et al., 2009) and secondary organic aerosols (SOA) (Kanakidou et al., 2005).

To get a more realistic picture on the causality of these effects, chemistry-transport models (CTMs) are systematically being used by the scientific community. CTMs are initialized with emission databases that provide a gridded and temporal representation of the emission fluxes of both anthropogenic and natural activity (Markakis et al., 2010). In order to compile such databases the parameterization of the natural processes that govern the emission is required. These mathematical expressions are voluminous in the published literature; for WD (Marticorena and Bergametti, 1995; Shao and Lu, 2000), SSA (Monahan et al., 1986; Sofiev et al., 2011), PBAPs (Vogel et al., 2008; Winiwarter et al., 2009) and BVOCs (Guenther et al., 1999; Muller et al., 2008). Some of these formulations are already integrated in CTMs; the DEAD model (Zender et al., 2003), CHIMERE-DUST (Menut et al., 2007), LOTOS-EUROS (Schaap et al., 2009), SILAM (Sofiev et al., 2011), CMAQ model (Mueller et al., 2011), CAMx-PM (Athanasopoulou et al., 2008, 2010) and the EMEP MSC-W model (Simpson et al., 2012). Air quality applications inherit the biases that stem from the inaccurate representation of natural emissions; emission models are based on empirical or semi-empirical methodologies (limited by the conditions under which they have been developed) as well as on the accuracy of the modelled meteorology.

This study presents a new natural emissions model (NEMO). NEMO is developed to provide the community with a software package that hosts state of the art methodologies for the quantification of emissions coming from the natural environment. We integrate parameterizations shown to improve air quality modeling applications. Up to now these methodologies are either implemented separately for each emission source or assimilated in photochemical models (SILAM, LOTOS-EUROS). Due to lack of integrated packages, such as NEMO, the modelling community often relies in off-line natural emissions databases that are inconsistent with the meteorological forcing of the air-quality modelling applications. Consequently, NEMO provides spatial (down to 1 km horizontal resolution) and temporal (down to hourly analysis) PM (WD, SSA and PBAPs) and BVOCs (vegetation) emissions suitable for photochemical modelling applications in Europe. The parameterizations implemented, input data, model structure and procedures are described in Section 2. In Section 3, results from an application of NEMO at European scale with 30 km horizontal resolution for the year 2009 are presented and discussed in comparison with meteorology. The above configuration is implemented in a modelling exercise with the photochemical Comprehensive Air Quality Model with extensions (CAMx). CAMx output PM concentrations are evaluated through a comparison with ground station measurements (Section 4). Section 5 summarizes the conclusions of the study.

2. Model description

NEMO is developed in Fortran90 and can be executed on a Linux PC. The mesoscale numerical Weather Research and Forecasting (WRF) model provides the meteorological fields (listed in the supplementary material) necessary for the emission calculations. The standard output of NEMO consists of a set of ACSII files that include the gridded and hourly (in gr/hour) resolved emissions of SSA (PM10 and PM2.5), WD (PM10 and PM2.5), PBAPs (PM10) and BVOCs (isoprene, monoterpenes and other VOCs). NEMO can be implemented in three different projections; Universal Transverse Mercator, Latitude/Longitude or Lambert Conic Conformal projection. For BVOCs, the calculation methodology is based on the work of Poupkou et al. (2010) which is updated here to include additional corrections that account for the leaf age (Guenther et al., 1999), soil moisture (Muller et al., 2008) and seasonality of emission rates (Steinbrecher et al., 2009). This paper focuses on the PM component of the model; BVOCs emission results are not presented in this study as a detailed analysis and evaluation of the BEM has been already described in Poupkou et al. (2010) while the efficacy of the refinements of the BVOCs module within NEMO will be the focus of future work.

2.1. Model structure and input databases

The model consists of four major subroutines which run in sequential order (Fig. 1); landgrid reprojects maps (land use, soil texture) from their native projection to the user-defined projection, readwrf develops appropriate WRF data to the output grid, nat-fields interpolates a number of key parameters (e.g. percentage sea coverage, vegetation reduction factor, dust coverage area etc.) to the output grid and natemissions performs the calculation of emissions.

NEMO requires the characterization of the vegetation and soil type, texture and clay fraction of particles in the soil, linked to the surface land-use. The latter is provided by the Eurasia Land Cover Characteristics database (version 2) freely distributed by the United States Geological Survey (USGS) (http://edc2.usgs.gov/glcc/eadoc2_0.php) in 1 km² spatial resolution. The landgrid subroutine reprojects the land use map to the user-defined projection in order to process with the emissions estimations. USGS includes 253 classifications of Land Use and Land Cover (LULC). The dust producing LULC classifications are barren land, grassland, cropland and agricultural land (156 in total). Forests, ocean surfaces as well as snow-covered areas have been excluded, as they are not considered significant dust sources (Ginoux et al., 2012). The soil texture database used in NEMO is compiled using a hybridization of two different sources of information. The European Soil Map database (ESDB) version 2.0 (Van Liedekerke and Panagos, 2006) at 100 m resolution which covers all EU25 countries, was extended to non-European neighbouring territory such as Turkey which is usually included in the European modelling domains, utilizing the global soil database of the Oak Ridge National Laboratory Distributed Active Archive Center (ORNL DAAC) (Webb et al., 2000) at 1° resolution (available at <http://www.daac.ornl.gov>). The two soil maps have been consolidated into a 6 km resolution database using a Geographical Information System (GIS). Having this as input, landgrid reprojects to the user-defined projection. The clay fractions of each texture class were derived from Chatenet et al. (1996) reclassified according to Schaap et al. (2009).

2.2. Emission model parameterizations

2.2.1. Windblown dust

The dust emission scheme of NEMO includes the

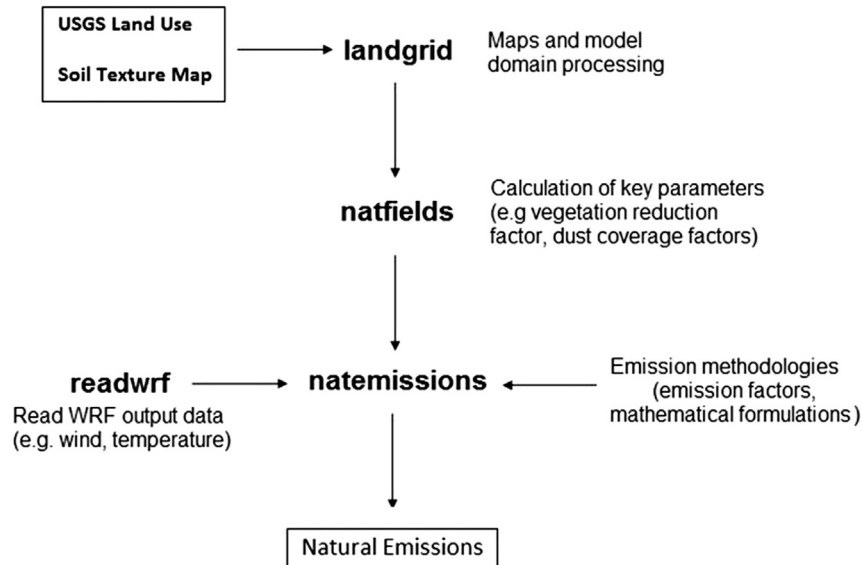


Fig. 1. Flowchart of NEMO.

parameterization of two processes: saltation (horizontal motion) and suspension (vertical motion) and it is based on the LOTOS-EUROS model (Schaap et al., 2009). The emission strength E_{dust} (g h^{-1}) depends on the size, the amount as well as the kinetic and binding energies of the saltating particles (Alfaro et al., 1997):

$$E_{DUST} = F_{V,i} \cdot A \cdot dt \quad (1)$$

where $F_{V,i}$ ($\text{g m}^{-2} \text{s}^{-1}$) is the vertical suspension flux, A (m^2) is the emitting area and dt is the time resolution of the model (in hours). $F_{V,i}$ is thoroughly described in Schaap et al. (2009) and it is a function of the total horizontally saltating mass flux (Eq. S.1 in supplement) of large particles which depends on the threshold friction velocity. NEMO implements three parameterizations of the threshold friction velocity in terms of soil particle size, drag partitioning and soil moisture according to Marticorena and Bergametti (1995) and Fecan et al. (1999).

In NEMO, constant values of the aerodynamic roughness length of bare soil including the non-erodible elements (z_0) and the smooth roughness length of the soil surface without any non-erodible elements (z_{0s}) were used according to the assumption of Zender et al. (2003); $z_0 = 0.01 \text{ cm}$, $z_{0s} = 0.0033 \text{ cm}$. Moreover, the formulation describing the drag partitioning has been modified according to Shinoda et al. (2011). Also, the parameterization of Fecan et al. (1999) was modified similarly to Athanasopoulou et al. (2010) in order model estimations to be improved; the threshold soil moisture was multiplied with 1.5.

Finally, criteria of non-emitting conditions are established in NEMO; surface temperature should be higher than 0°C for at least 12 h and no precipitation event prior to a period of 72 h (Korcz et al., 2009). During precipitation dust is not emitted.

2.2.2. Sea salt aerosols

SSA under $10 \mu\text{m}$ in diameter are emitted when wind stress disturbs a water surface capable of whitecap formation. The formulation implemented in NEMO in order to estimate emissions of SSA is mainly based on the methodology described in Sofiev et al. (2011) founded on the parameterizations of Monahan et al. (1986) and Martensson et al. (2003) aiming to introduce a synthesis relationship to account for the effect of wind stress, sea surface temperature (SST) and water salinity for a custom range of particle

sizes. The upward number flux of SSA dF/dD_p near the ocean surface per dry particle diameter D_p (μm) is estimated as (Sofiev et al., 2011):

$$\frac{dF}{dD_p} = \frac{dF_0}{dD_p} \cdot F_{Tw} \cdot F_{Sw} \cdot W \quad (2)$$

where dF_0/dD_p ($\text{m}^{-2} \text{s}^{-1} \mu\text{m}^{-1}$) is the reference number flux at a standard temperature and water salinity (3.3%) and F_{Tw} , F_{Sw} are correction factors to account for the SST and the salinity of water (the salinity values used in NEMO are given in supplement), respectively. W (dimensionless) is portion of unit area of water covered by whitecaps (Sofiev et al., 2011). The formulations of dF_0/dD_p as well as the correction factor F_{Tw} described in Sofiev et al. (2011) had been estimated at a reference temperature of 25°C . However, in the current study, updated formulations estimated in terms of a standard temperature of 20°C have been used (J. Soares, personal communication; Soares et al., 2015). Moreover, we utilize the equations of Lewis and Schwartz (2006), similarly to Sofiev et al. (2011), introducing the growth factor C^0 (Eq. S.2 in supplement).

In order to derive the particle mass from the estimated flux, we used the equations described in Zhang et al. (2005) considering particles to be perfect spheres and that the water salinity of the wet particle is equal to that of the water body of release. The particle mass is estimated as the product of its volume and density. Finally, for relative humidity greater than 45%, in order to obtain the dry particle mass, we used the formulation described in Zhang et al. (2005), which relates the solute weight fraction of SSA with ambient relative humidity.

2.2.3. PBAPs

PBAPs consist of a wide range of materials such as plant debris, fungal spores, pollen, bacteria and viruses (Bauer et al., 2002) from which only plant debris and fungal spores are considered in NEMO provided their large contribution in the PM10 mass (Winiwarter et al., 2009). The methodology implements two different emission factors that express the annual mass of particles emitted per unit area ($6 \text{ kg/km}^2/\text{year}$ for plant debris and $18 \text{ kg/km}^2/\text{year}$ for fungal spores) and it is independent of the surface type or vegetation (emissions are zero in water bodies, barren land and burned areas) (Winiwarter et al., 2009). The entrainment of PBAPs into the

atmosphere is described by the following equation:

$$E_{PBAPS} = (EF_{debris} \cdot t_{debris} + EF_{spores} \cdot t_{spores}) \cdot A \cdot dt \quad (3)$$

where E_{PBAPS} (in $\text{g} \cdot \text{h}^{-1}$) is the emission of PBAPs, EF_{debris} and EF_{spores} (in $\text{g m}^{-2} \text{ year}^{-1}$) are the emission factors for plant debris and fungal spores respectively, t_{debris} and t_{spores} are the temporal factors (in years) (see details in [supplement](#)) of plant debris and fungal spores, respectively, A (in m^2) is the emission (grid cell) area and dt is the time unit of the simulation (in hours).

3. NEMO application and results

3.1. Model application

NEMO was used to derive natural emissions over a 30 km horizontal resolution grid covering Europe and the adjacent areas (i.e. Turkey, Syria, Lebanon, Israel and Jordan) ([Fig. 3](#)). The output grid consisted of 141 columns by 134 rows projected in Lambert Conic Conformal (LCC). The hourly meteorological data used for driving NEMO were derived from the WRF model, version 3.5.1 ([Skamarock et al., 2008](#)). For the initialization of WRF the 6 h temporal resolution and $0.5^\circ \times 0.5^\circ$ spatial resolution operational atmospheric analyses surface and pressure level data of the European Centre for Medium-range Weather Forecasts (ECMWF) were used.

3.2. Emissions results and discussion

This section presents the estimated domain-wide annual emissions of PM10 and PM2.5 for the year 2009 ([Table 1](#)) and their

temporal and spatial variation ([Figs. 2–5](#)). The monthly spatial distribution of emissions is presented for winter, summer and autumn for the months with the highest emissions: January, July, October (for WD) and November (for SSA). The lowest seasonally emissions are found in spring and therefore month April (lowest monthly emissions of the year) was selected. PM2.5 emissions have a similar temporal and spatial distribution with that of PM10 and therefore they are not presented.

The total PM10 mass emitted from WD in the domain is estimated to be 0.57 Tg with the majority emitted in the coarse mode; PM2.5 emissions contribute by 6%. [Korcz et al. \(2009\)](#) had estimated a best average value of 0.88 Tg/year of PM10 WD emissions over Europe and a part of Southwest Asian (similar area with that of the current study) for the period 2000–2003 while [NATAIR \(2007\)](#) presented an estimated uncertainty of a factor of 12 for WD emissions. WD emissions are very sensitive to the precipitation rates and therefore their emissions are mainly limited to the southern Europe attributed to the drier climate in combination with high wind speed values. WD emissions are the highest during summer with a peak in July ([Fig. 2a](#)) when the frequency of dust events in southern Greece and Spain, Turkey and Syria increases ([Fig. 4c](#)) where mean soil moisture is the lowest ($<0.24 \text{ m}^3/\text{m}^3$). In addition, the high wind speed values (6–9 m/s) over the Eastern Mediterranean in July, contribute to high PM10 emissions. Similarly, in October, a lot of dust episodes are identified in Turkey and southern Greece where mean soil moisture is minimum, but with lower intensity ($<1 \text{ tn}/\text{km}^2$) due to the moderate wind speed values (5–6 m/s). During winter and spring, sparse WD events occur over the southern Europe where mean monthly soil moisture is lower than $0.3 \text{ m}^3/\text{m}^3$. However, the strong wind speeds in winter and in

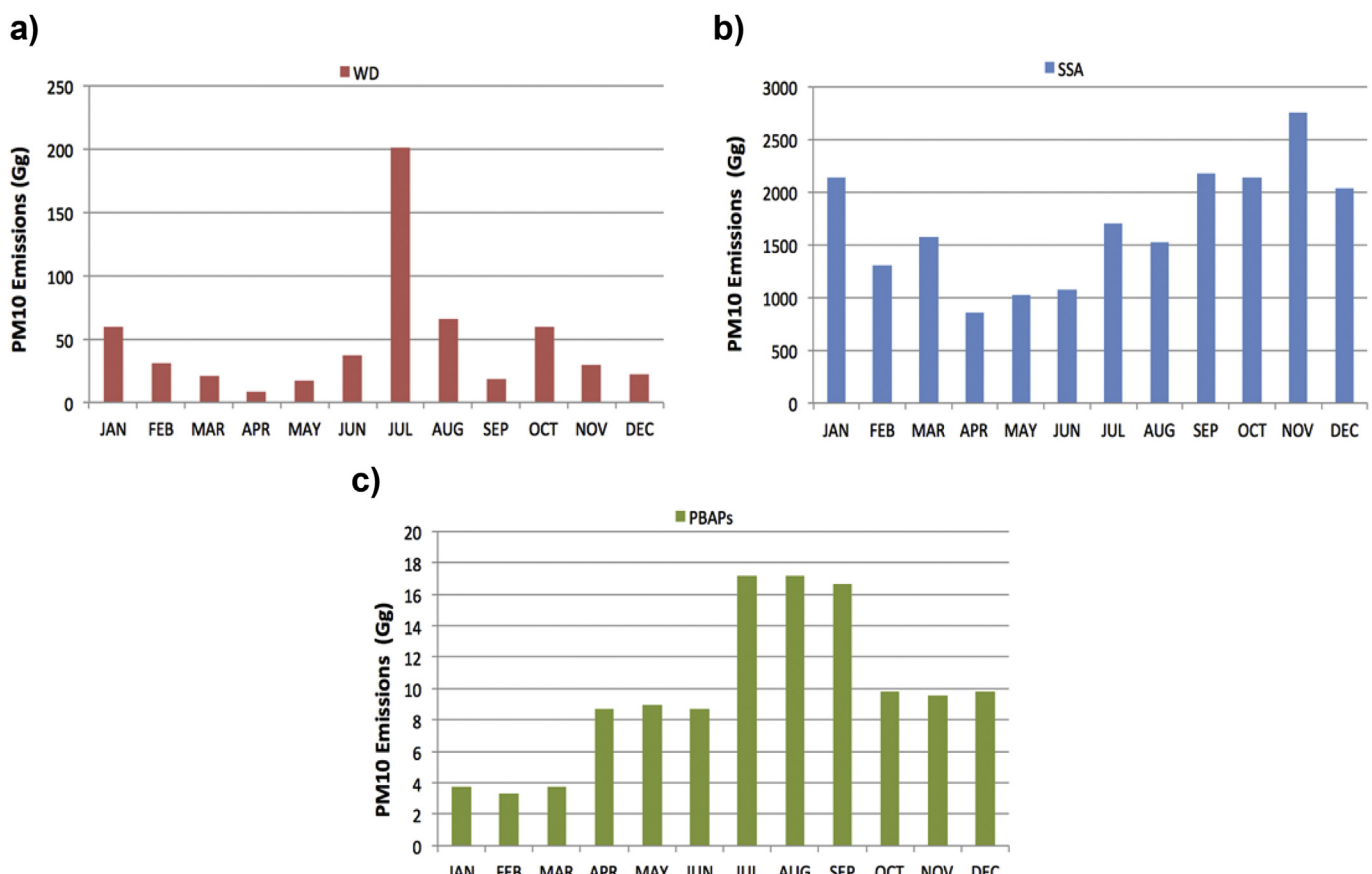


Fig. 2. Monthly variation of PM10 emissions (Gg/month) from a) WD, b) SSA and c) PBAPs over the study area (Europe and adjacent areas, [Fig. 3](#)) in 2009.

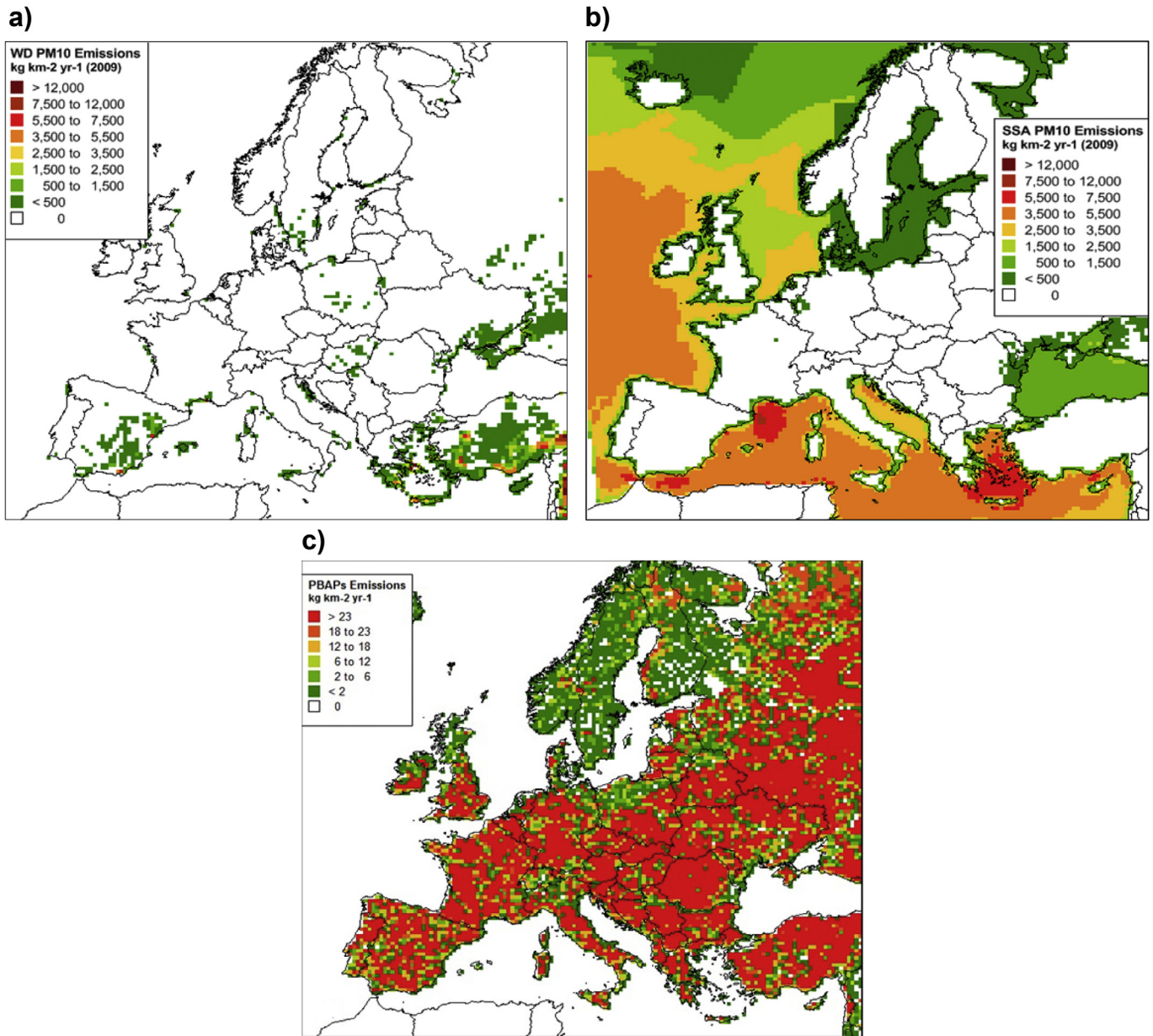


Fig. 3. Spatial distribution of annual PM10 emissions (kg/km^2) from a) WD, b) SSA and c) PBAPs over the study area in 2009.

Table 1
Annual PM emissions from natural sources in the study area (Fig. 3) in 2009.

Emission source	Annual PM emissions (Gg)	
	PM10	PM2.5
Windblown dust	572	34
Sea salt aerosols	20308	6863
PBAPs	117	—

particular in January, lead to intense dust episodes in Turkey ($>4.5 \text{ tn}/\text{km}^2$).

Annual domain-wide SSA PM10 emissions are estimated as 20 Tg (dry mass), 33% of which is attributed to the fine mode. A lower amount of around 4.4 Tg of SSA emissions had been estimated by NATAIR (2007) over Europe for the year 2003. However, several studies in the past have revealed high uncertainties in sea salt emissions estimations (Schaap et al., 2009; NATAIR, 2007). The

highest PM10 mass over the study area is emitted during autumn and winter with the majority of them emitted in November. This peak is attributed to the high SSA emissions ($>1 \text{ tn}/\text{km}^2$) over a portion of the Atlantic Ocean where wind speed peaks ($>12 \text{ m/s}$). During summer, emissions are the highest in Mediterranean Sea due to the warmer seas ($>20^\circ\text{C}$), being the highest in the Aegean Sea ($>1 \text{ tn}/\text{km}^2$), which is characterized by high wind speed values (7–9 m/s). Emissions are also high ($>450 \text{ kg}/\text{km}^2$) over the Balearic Sea where moderate wind speeds are found (5–6 m/s). In spring, SSA production is not important as wind speed and water temperature values are moderate. In the northern part of Atlantic Ocean the mean wind speed is very high ($>12 \text{ m/s}$) but the very low SST values ($<10^\circ\text{C}$) result to minimum SSA emissions. The lowest values of SSA emissions through the year are found in the Baltic and Black Seas due to their very low water salinity.

PBAPs emissions in NEMO are estimated as 0.12 Tg (a comparable estimate of 0.15 Tg over Europe in 2003 is given in NATAIR

Table 2

Mean observed and simulated PM10 mineral dust concentrations ($\mu\text{g}/\text{m}^3$) for the cold (C) and warm (W) periods of the year 2009.

Site name	Obs. Mean ($\mu\text{g}/\text{m}^3$)		Sim. Mean ($\mu\text{g}/\text{m}^3$)		Sim./Obs. Mean		σ_o		σ_s		BIAS ($\mu\text{g}/\text{m}^3$)		IOA	
	C	W	C	W	C	W	C	W	C	W	C	W	C	W
Finokalia	17.06	4.25	7.95	3.61	0.47	0.85	42.89	4.90	10.90	3.65	-9.10	-0.64	0.49	0.63
Corso Firenze	3.97	4.97	3.63	2.74	0.92	0.55	2.45	2.94	4.22	3.40	-0.34	-2.23	0.76	0.64
Campi-sabalos	1.84	3.99	2.32	3.00	1.26	0.75	2.25	2.84	4.52	3.19	0.48	-0.99	0.58	0.63
Montseny	2.59	4.92	1.75	2.93	0.68	0.60	2.59	3.82	2.46	3.17	-0.84	-1.98	0.61	0.68
Melpitz	0.85	0.93	2.17	1.60	2.54	1.72	0.72	0.53	2.40	1.36	1.32	0.67	0.32	0.40
Harwell	1.91	0.34	2.56	1.46	1.34	4.23	2.12	0.59	2.62	1.24	0.66	1.12	0.66	0.21
Auchencorth Moss	1.16	1.34	0.79	0.99	0.68	0.74	1.02	1.72	0.93	0.78	-0.38	-0.35	0.36	0.42
Mean	4.20	2.96	3.02	2.33	0.72	0.79	7.72	2.48	4.01	2.40	-1.17	-0.63	0.54	0.52

Table 3

Mean observed and simulated PM2.5 sodium (Na) concentrations ($\mu\text{g}/\text{m}^3$) for the cold (C) and warm (W) periods of the year 2009.

Site name	Obs. Mean ($\mu\text{g}/\text{m}^3$)		Sim. Mean ($\mu\text{g}/\text{m}^3$)		Sim./Obs. Mean		σ_o		σ_s		BIAS ($\mu\text{g}/\text{m}^3$)		IOA	
	C	W	C	W	C	W	C	W	C	W	C	W	C	W
Agia Marina	0.40	0.30	0.57	0.69	1.42	2.31	0.31	0.23	0.34	0.42	0.17	0.39	0.38	0.18
Corso Firenze	0.20	0.28	0.55	0.63	2.69	2.28	0.19	0.22	0.32	0.50	0.35	0.35	0.56	0.34
Mace Head	0.65	0.38	0.76	0.72	1.17	1.87	0.45	0.26	0.24	0.29	0.11	0.34	0.65	0.47
Harwell	0.68	0.62	0.65	0.67	0.96	1.07	0.71	0.70	0.45	0.37	-0.03	0.04	0.51	0.28
Auchencorth Moss	0.65	0.75	0.62	0.61	0.95	0.81	0.60	1.13	0.35	0.37	-0.03	-0.15	0.52	0.22
Rucava	0.78	5.41	0.32	1.35	0.40	0.25	0.86	10.12	0.22	2.60	-0.47	-4.05	0.42	0.37
Zoseni	0.67	0.09	0.26	0.26	0.38	3.02	0.69	0.05	0.14	0.15	-0.41	0.17	0.41	0.37
Mean	0.58	1.12	0.53	0.70	0.91	0.63	0.54	1.82	0.29	0.67	-0.04	-0.42	0.49	0.32

(2007)) being the highest from July to September due to the highest emission factors of the period July–September used for the estimations. Minimum PM10 emissions are found during wintertime (January to March). PBAPs emissions are lowest in Scandinavia while they have an equal distribution over the rest study area (Fig. 3c). The pattern of the spatial distribution of the monthly emissions is similar with that of the annual spatial distribution (Fig. 3c) and therefore it is not presented.

4. Model evaluation

The gridded emissions of PM and BVOCs calculated with NEMO and presented in the previous section were used as input in a modelling application with the CAMx model (version 5.3) (ENVIRON, 2010) in order to evaluate NEMO through a comparison with measurement aerosol data.

4.1. Modelling system

The CAMx application and NEMO share identical meteorological drivers and modelling domains. In the present study, dust emissions were simulated in CAMx runs as fine and coarse crustal particle emissions. Fine SSA emissions were split into particulate chloride (55.04%), sodium (30.61%), sulfates (7.68%) and other primary fine particles (6.67%) emissions (Seinfeld and Pandis, 2006). Coarse SSA emissions were simulated as other primary coarse particles. SSA concentrations could be traced in CAMx output data as fine particulate chloride and sodium concentrations since sulfates and other primary particles (fine or coarse) levels were determined also by the anthropogenic contribution.

Average concentrations derived from the Integrated Forecasting System (IFS) MOZART model (Morcrette et al., 2009; Inness et al., 2013) as well as average monthly SSA concentrations taken from the EMEP MSC-W chemical transport model (Simpson et al., 2012) for the year 2009 were used as boundary conditions (BCs) for the simulations.

4.2. Anthropogenic emission data

Anthropogenic emission data for Europe were taken by the TNO-MACCII emission database for the year 2009 (Kuenen et al., 2014) which was temporally and spatially analysed using the Model for the Spatial and Temporal Distribution of Emissions (MOSESS) (Markakis et al., 2013). Annual potential particle emissions of mineral dust from re-suspension due to traffic circulation as well as 12 monthly potential mineral dust emissions from agricultural activities, estimated using the LOTOS-EUROS model (Schaap et al., 2009), were provided by The Netherlands Organisation (TNO). They were temporally analysed using the temporal profiles given by TNO (Schaap et al., 2009), taking also into account meteorological restrictions using the 2009 hourly WRF meteorological data i.e. dust emissions were forced to zero during precipitation events.

It should be taken into account that anthropogenic mineral dust emissions pose uncertainties in dust emissions estimations over the whole study area due to the assumptions that have been made for the calculations according to Schaap et al. (2009).

4.3. Measurement data

Measurement data were taken either from the European Monitoring and Evaluation Programme (EMEP) monitoring network (<http://ebas.nilu.no>) or from national networks (Table S1, Fig. S4 in supplement). The validation was performed for the year 2009. A comparison of the statistical measures (description is given in supplement) during a cold (November to April) and a warm (May to October) period of the year is presented.

4.4. Comparison between simulated and observed PM10 dust concentrations

Simulated PM10 mineral dust concentrations (including its natural and anthropogenic components) are compared with the

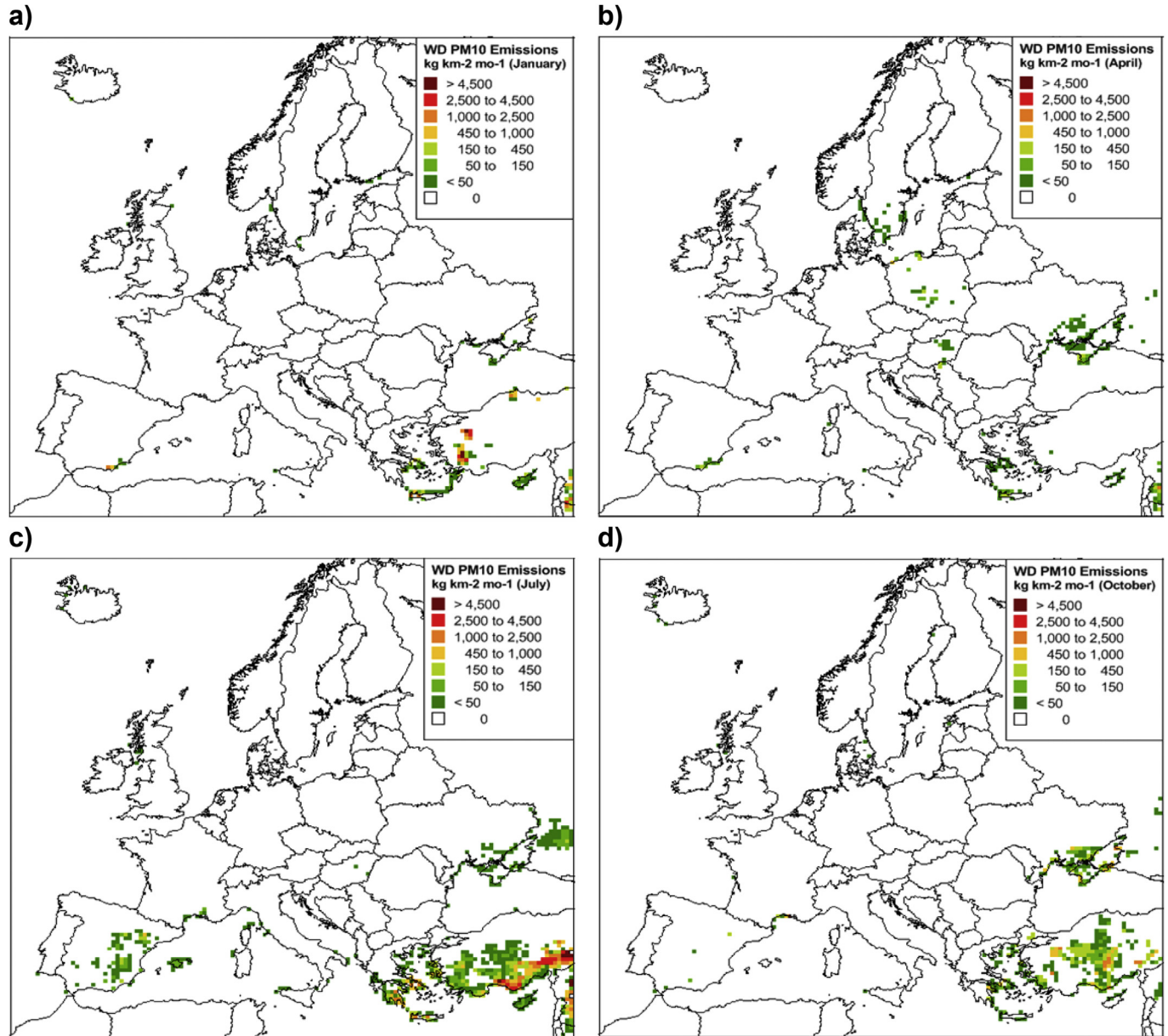


Fig. 4. Spatial distribution of monthly PM10 windblown dust emissions (kg/km^2) for a) January, b) April, c) July and d) October of 2009 over the study area.

corresponding observed ones. Only the site of Finokalia provided directly with dust concentrations. For two sites (Corso Firenze and Montseny), dust concentrations were calculated using the concentrations of several elements inputted in the equation of Chan et al. (1997) (Eq. S3 in supplement). For the remaining sites for which only calcium (Ca) measurements were available, Ca was used as a soil dust tracer (Aas et al., 2012; Athanasiopoulou et al., 2010; Schaap et al., 2009). This was done by calculating the average ratio between the mean annual mineral dust PM10 concentrations and that of Ca. In the current study, the corresponding ratio was 7, 6.8 and 9.8 for Corso Firenze, Finokalia and Montseny sites, respectively. Thus, for the monitoring sites in which only Ca measurements were available, a ratio of 7.5 (Schaap et al., 2009) was used in order to estimate PM10 mineral dust concentration. Regarding PM2.5 concentrations, WD PM2.5 emissions represent only a 6% share of PM10 emissions and therefore their evaluation is not examined.

On average for all sites, the model underestimates by 28% and 20% PM10 dust concentrations for the cold and warm period, respectively (see Table 2). The average bias (Eq. S5 in supplement) for PM10 dust concentrations takes small negative values for both periods with a better performance in the warm period. On annual basis, the corresponding underestimation of PM10 dust concentrations is 28% (Table S2, in supplement). Given that windblown dust emissions in Europe show a high uncertainty of a factor of 12 (NATAIR, 2007), modelled results are satisfactory. Moreover, for monitoring stations for which PM10 dust concentrations were derived from the ratio between PM10 and Ca concentrations, an uncertainty in model evaluation is also expected.

In the eastern Mediterranean, in Finokalia station, the model performance is better during the warm period compared to the cold one. According to the total PM10 measurement data provided by Finokalia, some dust transport episodes occurred mainly during January to March (PM10 levels were higher than $100 \mu\text{g}/\text{m}^3$) have

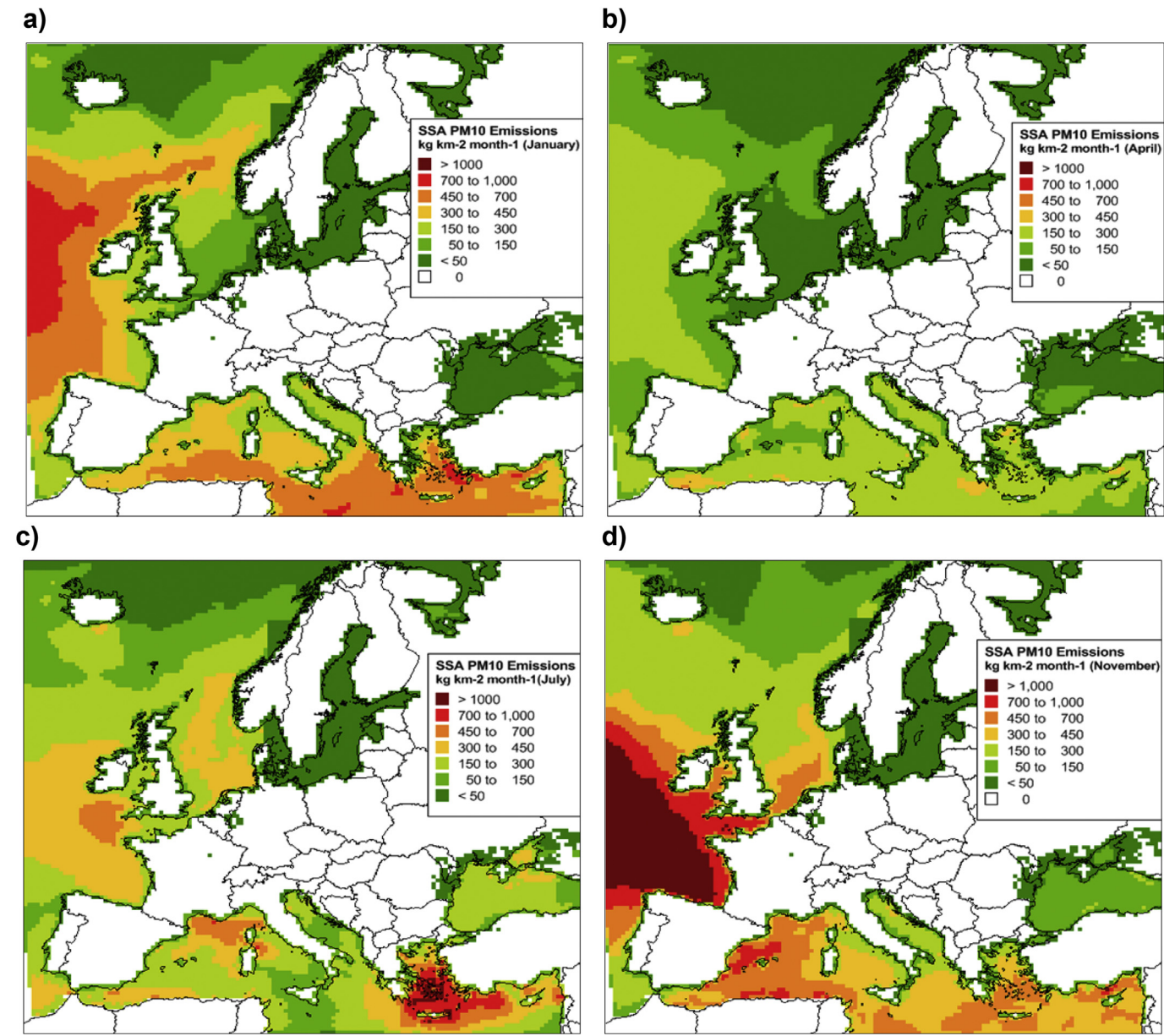


Fig. 5. Spatial distribution of monthly PM10 SSA emissions (kg/km^2) for a) January, b) April, c) July and d) November of 2009 over the study area.

probably not been well captured by BCs (Cansado et al., 2014) resulting to a low model performance during the cold period. During the warm season, an underestimation of 15% in PM10 dust concentrations and an Index of Agreement (IOA) (Eq. S6 in supplement) of 0.63 indicate a very good model performance when dust transport events are absent.

In the western and central Mediterranean (Spain and Italy, respectively), there is an improvement in PM10 dust concentrations during the cold season in the absence of Sahara dust events (Pey et al., 2013). At Corse Firenze site, a BIAS of $-0.34 \mu\text{g}/\text{m}^3$ in the cold period is estimated in PM10 values with an IOA of 0.76 indicating a very good model performance. In Montseny, according to the standard deviations of the simulated and observed PM10 dust concentrations, the model slightly underestimates the variability of the observed PM10 values in both periods.

In central and northern Europe, in Melpitz site, there is an improvement in model performance during the warm period. The area around Melpitz is characterized by high agricultural dust

emissions, which have been highly overestimated mainly during March and April (Schaap et al., 2009) explaining the corresponding overestimation of PM10 dust concentrations during the cold period. In Great Britain, Harwell site shows a good agreement between the observed and modelled PM10 concentrations in the cold period (IOA = 0.66). In Auchencorth Moss the PM10 results are satisfactory with a slight underestimation of dust concentrations in both periods and a BIAS of $-0.35 \mu\text{g}/\text{m}^3$ in the warm season.

Mean daily values of PM10 dust modelled levels agree within a factor of 3 for most of the daily values in the selected monitoring sites (Fig. 6) indicating a good agreement if taking into consideration the high levels of estimated uncertainty of windblown dust emissions (NATAIR, 2007). It seems that the model captures similarly well the higher and lower concentrations of the dust events except for those of the dust episodes associated with the Sahara dust transport from the boundaries (Fig. 6a), as it has already been discussed above.

In comparison with existing models, the model evaluation is

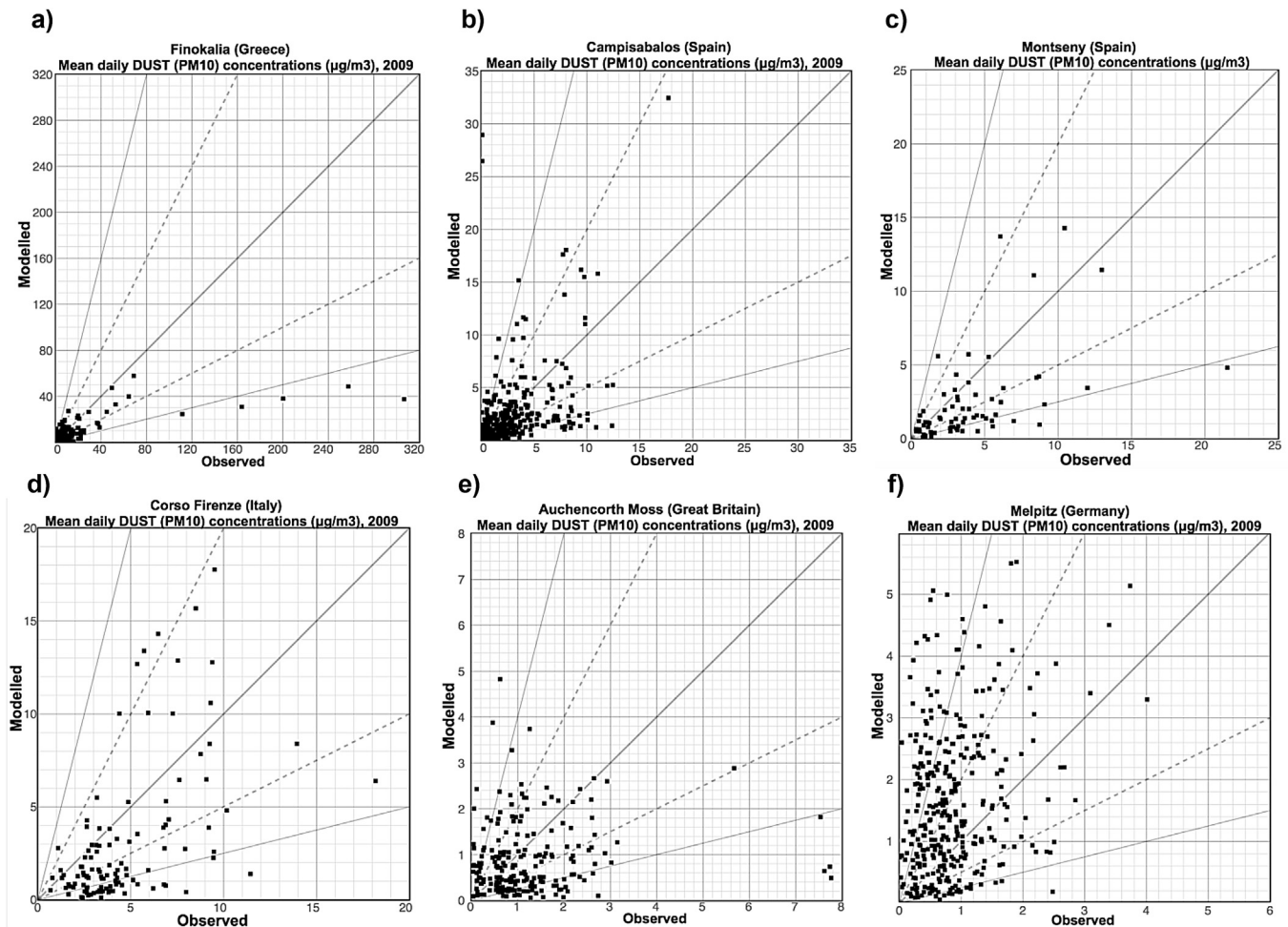


Fig. 6. Mean daily observed versus modelled dust PM10 concentrations ($\mu\text{g}/\text{m}^3$) for 2009 for selected monitoring sites.

good and in agreement with previous studies. In Schaap et al. (2009) the LOTOS-EUROS model was implemented and evaluated over Europe for 2005. In Melpitz site, a positive bias of $0.57 \mu\text{g}/\text{m}^3$ was estimated between the mean annual modelled and observed PM10 dust concentrations. A comparable bias is estimated in the current study ($0.99 \mu\text{g}/\text{m}^3$) (Table S2) for Melpitz site. In Montseny, Schaap et al. (2009) found a bias of $0.07 \mu\text{g}/\text{m}^3$ for dust concentrations while a quite higher underestimation is presented in the present study with a bias of $-1.40 \mu\text{g}/\text{m}^3$.

4.5. Comparison between simulated and observed PM2.5 sodium concentrations

Typically, sodium is considered as a tracer of sea salt (Tsyro et al., 2011) and used for the evaluation of modelled SSA concentrations. From the CAMx simulations, only PM2.5 SSA concentrations were available and therefore the evaluation of sea salt concerns only that particular bin.

On average for all sites located in Atlantic Ocean and Mediterranean Sea, the model overestimates sodium concentrations by 22% and 42% in the cold and warm period, respectively (see Table 3). On an annual basis, an overestimation of around 31% has been found. In Baltic Sea, an annual underestimation of 36% in sodium concentrations is found. According to Schaap et al. (2009), the uncertainty in sea salt concentrations was considered to be of a factor of 2–3 while in NATAIR (2007) the estimated uncertainty ranged from a factor of 2–4 suggesting that NEMO captured fairly well the SSA episodes.

SSA production is well captured mostly in the stations located close to the Atlantic Ocean. In Mace Head, the mean modelled sodium concentrations in the cold season are of the same order of magnitude as the observed ones while the values of 0.65 and $0.11 \mu\text{g}/\text{m}^3$ for IOA and BIAS, respectively are satisfactory. The statistical scores of the two stations located in Great Britain show that there is a very good agreement between the simulated and observed data for both periods.

Rucava and Zoseni are close to Baltic Sea where the water salinity is very low resulting to very low SSA emissions and therefore an underestimation of Na concentrations is shown.

In Mediterranean Sea, in Agia Marina site, a mean BIAS of $0.17 \mu\text{g}/\text{m}^3$ has been calculated for the cold period while the values of standard deviation of observed and simulated sodium concentrations are similar showing a slight tendency to overestimate PM2.5 (Na) values. A larger overestimation is presented in the warm season. In Corso Firenze, the model overestimates the observed sodium concentrations while the mean IOA in cold season is estimated as 0.56. The observed overestimation of SSA concentrations in the warm period suggests uncertainties in the SST parameterization.

The mean daily sodium modelled versus observed concentrations are presented in Fig. 7 for the sites for which daily data were available. The modelled results agree within a factor of 2 for most of the days with the observation data in the selected sites except for the site of Corso Firenze for which an uncertainty within a factor of 4 was estimated. The estimated uncertainties are in the range of

those calculated in previous studies (NATAIR, 2007; Schaap et al., 2009).

In comparison with existing models, the model captures better the SSA episodes in selected areas. In particular, sea salt concentrations had been estimated with the LOTOS-EUROS model (Schaap et al., 2009) over Europe for 2005. They found a bias of $-1.1 \mu\text{g}/\text{m}^3$ in mean annual sodium concentrations at Valentia Observatory site, which is located in Ireland, facing the North East Atlantic Ocean. In the same site, in the study of Tsyro et al. (2011), the evaluation of EMEP and SILAM models for the year 2007 showed a bias of $+0.6 \mu\text{g}/\text{m}^3$ and $-0.16 \mu\text{g}/\text{m}^3$. In the current study, in the site of Mace Head, which is also located in Ireland facing the North East Atlantic Ocean, a bias of $+0.24 \mu\text{g}/\text{m}^3$ has been estimated indicating a very good model performance. Also, Schaap et al. (2009), found a large overestimation of sodium concentrations ($\sim 170\%$) for Rucava site. NEMO estimations led to an underestimation of 36% in the corresponding sodium concentrations.

5. Conclusions

A new emission model, NEMO, has been described, implemented on a photochemical modelling system and evaluated through a comparison between the simulated and observed data. NEMO is a robust model, which has been developed in order to provide scientific community with a single software package that

integrates well-documented methodologies and parameterizations for natural emissions estimations and incorporating in CTMs improving air quality simulations.

An application of NEMO in a 30 km spatial resolution grid covering Europe was presented for the year 2009. The dry climate of southern Europe during summer, mostly in Greece and Turkey, in combination with the moderate wind speed values led to maximum WD emissions in those areas during summer. The strong winds in a portion of Atlantic Ocean in combination with the moderate sea temperatures led to high SSA emissions during autumn. In summer, SSA emissions peaked in Mediterranean Sea due to the warmer seas while they were highlighted in Aegean Sea where wind speed peaks.

The natural PM emission data were used in an application of the WRF-CAMx modelling system. The model captured fairly well the WD emission events while there was a better performance when dust transport episodes from Sahara desert were absent. NEMO captured very well the sea salt episodes in Atlantic Ocean. In Mediterranean Sea, a good model performance has been shown with an improvement in cold season. The model overestimated sodium concentrations in the warm season mainly in sites located in the Mediterranean Sea due to the higher SST values. In sites located close to Baltic Sea that is characterized by very low salinity values, a slight underestimation was shown.

In conclusion, NEMO can be used for the estimation of natural

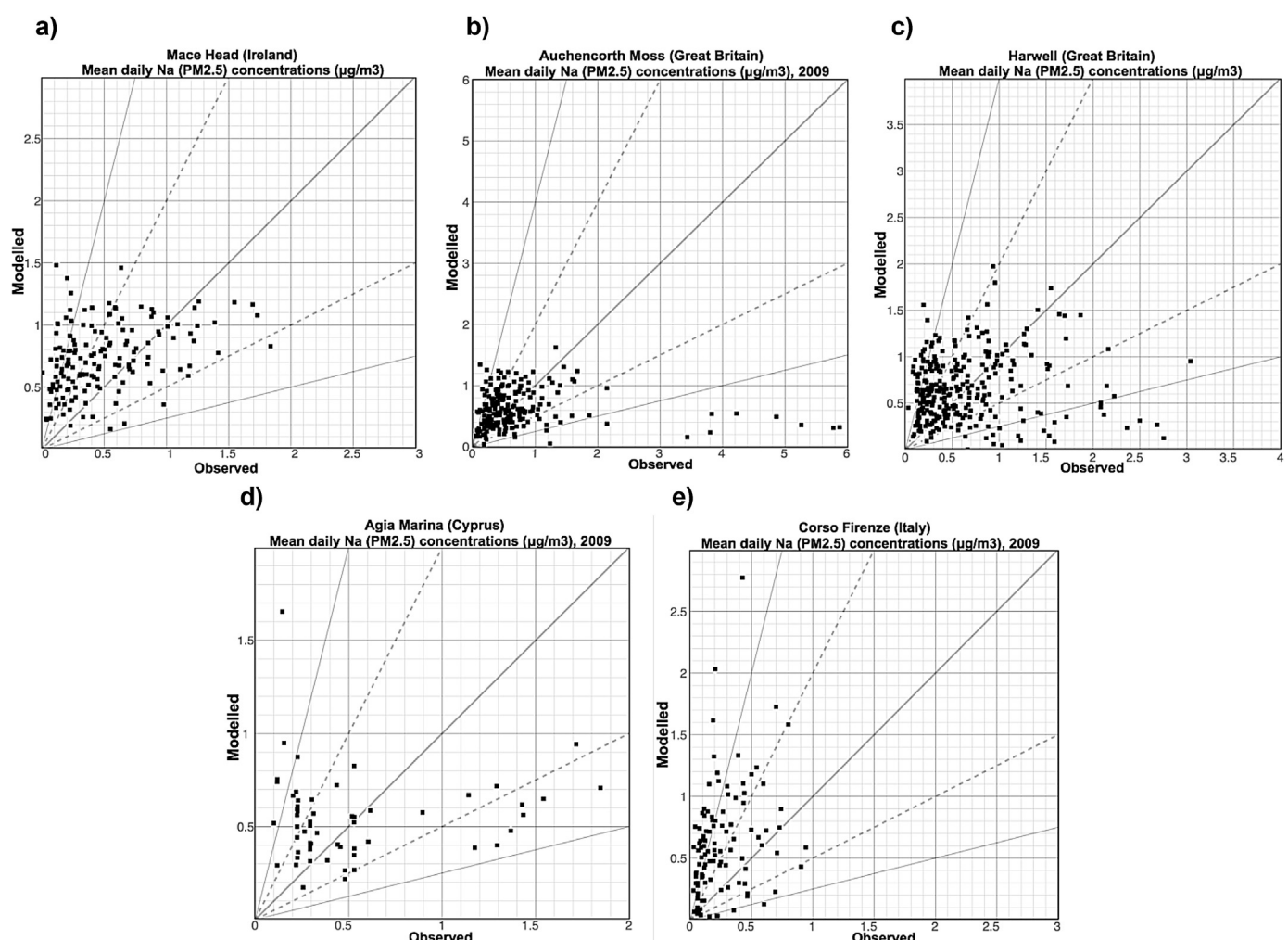


Fig. 7. Mean daily observed versus modelled sodium (PM2.5) concentrations ($\mu\text{g}/\text{m}^3$) for 2009 for selected monitoring sites.

emissions at European scale in order to be applied on photochemical models so as to improve air quality simulations. The evaluation of NEMO indicated a good model performance while the differences between the observed and simulated data, on an annual basis, were in agreement with previous studies. However, improvements must be done mostly in terms of SST parameterization for SSA emission estimations.

Acknowledgements

The present study has been supported by NPRP award number NPRP 7-649-2-241 from the Qatar National Research Fund (a member of The Qatar Foundation). The authors would also like to acknowledge the EU project MACC-III (Monitoring Atmospheric Composition and Climate - III, Horizon 2020, Grant agreement no: 633080). The results presented in this research paper have been produced using the EGI and HellasGrid infrastructures. The authors would like to acknowledge the support provided by the Scientific Computing Center at the Aristotle University of Thessaloniki throughout the progress of this research work. We thank Dr. D. Ceburnis, Dr. G. Kouvarakis, Mr. D. Massabo and Prof. P. Pratti and Dr. N. Perez, for the measurement data availability. We thank also Mr. M. Schaap and Mr. R. Kranenburg for providing the anthropogenic mineral dust emission data and Mrs. J. Soares for the availability of the updated functions for sea salt emissions estimations. We would like to thank for the IFS-MOZART data and TNO anthropogenic emission data provided in the framework of the MACC-II project (Monitoring Atmospheric Composition and Climate - Interim Implementation, Grant agreement no: 283576). Finally, we thank Dr. S. Tsyro for the EMEP-MSC-W data availability.

Appendix A. Supplementary data

Supplementary data related to this article can be found at <http://dx.doi.org/10.1016/j.atmosenv.2015.10.014>.

References

- Aas, W., Tsyro, S., Bieber, E., Bergstrom, R., Ceburnis, D., Ellermann, T., Fagerli, H., Frolich, M., Gehrig, R., Makkonen, U., Nemitz, E., Oties, R., Perez, N., Perrino, C., Prevot, A.S.H., Putaud, J.P., Simpson, D., Spindler, G., Vana, M., Yttri, K.E., 2012. Lessons learnt from the first EMEP intensive measurement periods. *Atmos. Chem. Phys.* 12, 8073–8094. www.atmos-chem-phys.net/12/8073/2012/doi:10.5194/acp-12-8073-2012.
- Alfaro, S.C., Gaudichet, A., Gomes, L., Maille, M., 1997. Modelling the size distribution of a soil aerosol produced by sandblasting. *J. Geophys. Res.* 102, 11239–11249.
- Athanasiopoulou, E., Tombrou, M., Pandis, S.N., Russel, A.G., 2008. The role of sea-salt emissions and heterogeneous chemistry in the air quality of polluted coastal areas. *Atmos. Chem. Phys.* 8, 5755e5769.
- Athanasiopoulou, E., Tombrou, M., Russell, A.G., Karanasiou, A., Eleftheriadis, K., Dandou, A., 2010. Implementation of road and soil dust emission parameterizations in the aerosol model CAMx: applications over the greater Athens urban area affected by natural sources. *J. Geophys. Res. D Atmos.* 115.
- Bauer, H., Kasper-Giebl, A., Ifflund, M., Giebl, H., Hitzenberger, R., Zibuschka, F., Puxbaum, H., 2002. The contribution of bacterial and fungal spores to the organic carbon content of cloud water, precipitation and aerosols. *Atmos. Res.* 64, 109–119.
- Cansado, A., Moreta, J.R., Lopez, E., Martinez, I., Melas, D., Avgoloupis, S., Poupkou, A., Katragkou, E., Giannaros, C., 2014. Evaluation of ENS Models in the Mediterranean Area. MACC-ii Project (Monitoring Atmospheric Composition and Climate - Interim Implementation), 2014. Deliverable D_106.29.
- Chan, Y.C., Simpson, R.W., McTainsh, G.H., Vowles, P.D., Cohen, D.D., Baily, G.M., 1997. Characterisation of chemical species in PM2.5 and PM10 aerosols in Brisbane, Australia. *Atmos. Environ.* 31, 3773–3785.
- Chatenet, B., Marticorena, M., Gomes, L., Bergametti, G., 1996. Assessing the microscopic size distributions of desert soils erodible by wind. *Sedimentology* 43 (5), 901–911.
- Curci, G., Beekmann, M., Vautard, R., Smiatek, G., Steinbrecher, R., Theloke, J., Friedrich, R., 2009. Modelling study of the impact of isoprene and terpene biogenic emissions on European ozone levels. *Atmos. Environ.* 43, 1444e1455.
- Dillon, H.K., Miller, J.D., Sorenson, W.G., Douwes, J., Jacobs, R.R., 1999. Review of methods applicable to the assessment of mold exposure to children. *Environ. Health Persp.* 107, 473–480.
- ENVIRON, 2010. User's Guide CAMx Comprehensive Air Quality Model with Extensions, Version 5.30. ENVIRON International Corporation. December 2010.
- ESDB v2.0: the European Soil Database Distribution Version 2.0, European Commission and the European Soil Bureau Network, CD-ROM, EUR 19945 EN, 2004.
- Fecan, F., Marticorena, B., Bergametti, G., 1999. Parametrization of the increase of the aeolian erosion threshold wind friction velocity due to soil moisture for arid and semi-arid areas. *Ann. Geophys.* 17 (1), 149–157.
- Ginoux, P., Prospero, J.M., Gill, T.E., Hsu, N.C., Zhao, M., 2012. Global-scale attribution of anthropogenic and natural dust sources and their emission rates based on MODIS deep blue aerosol products. *Rev. Geophys.* 50 <http://dx.doi.org/10.1029/2012RG000388>. RG3005.
- Guenther, A., Baugh, B., Brasseur, G., Greenberg, J., Harley, P., Klinger, L., Serca, D., Vierling, L., 1999. Isoprene emission estimates and uncertainties for the Central African EXPRESSO study domain. *J. Geophys. Res. Atmos.* 104 (D23), 30,625–30,639.
- Im, U., Markakis, K., Kocak, M., Gerasopoulos, E., Daskalakis, N., Mihalopoulos, N., Poupkou, A., Kindap, T., Unal, A., Kanakidou, M., 2012. Summertime aerosol chemical composition in the Eastern Mediterranean and its sensitivity to temperature. *Atmos. Environ.* 50, 164–173.
- Inness, A., Baier, F., Benedetti, A., Bouarar, I., Chabirillat, S., Clark, H., Clerbaux, C., Coheur, P., Engelen, R.J., Errera, Q., Flemming, J., George, M., Granier, C., Hadjilazaro, J., Huijnen, V., Hurtmans, D., Jones, L., Kaiser, J.W., Kapsomenakis, J., Lefever, K., Leitao, J., Razinger, M., Richter, A., Schultz, M.G., Simmons, A.J., Suttie, M., Stein, O., Thepaut, J.-N., Thouret, V., Vrekoussis, M., Zerefos, C., the MACC team, 2013. The MACC reanalysis: an 8 yr data set of atmospheric composition. *Atmos. Chem. Phys.* 13, 4073–4109. <http://dx.doi.org/10.5194/acp-13-4073-2013>.
- Kanakidou, M., Seinfeld, J.H., Pandis, S.N., Barnes, I., Dentener, F.J., Facchini, M.C., Van Dingenen, R., Ervens, B., Nenes, A., Nielsen, C.J., Swietlicki, E., Putaud, J.P., Balkanski, Y., Fuzzi, S., Horth, J., Moortgat, G.K., Winterhalter, R., Myhre, C.E.L., Tsigaridis, K., Vignati, E., Stephanou, E.G., Wilson, J., 2005. Organic aerosol and global climate modelling: a review. *Atmos. Chem. Phys.* 5, 1053e1123.
- Karanasiou, A., Moreno, N., Moreno, T., Viana, M., de Leeuw, F., Querol, X., 2012. Health effects from Sahara dust episodes in Europe: literature review and research gaps. *Environ. Int.* 47, 107–114.
- Korcz, M., Fudala, J., Clis, C., 2009. Estimation of windblown dust emissions in Europe and its vicinity. *Atmos. Environ.* 43, 1410–1420.
- Kuenen, J.J.P., Visschedijk, A.J.H., Jozwicka, M., Denier van der Gon, H.A.C., 2014. TNO-MACC_II emission inventory: a multi-year (2003–2009) consistent high resolution European emission inventory for air quality modelling. *Atmos. Chem. Phys. Discuss.* 14, 5837–5869. www.atmos-chem-phys-discuss.net/14/5837/2014/doi:10.5194/acpd-14-5837-2014.
- Lewis, E.R., Schwartz, S.E., 2006. Comment on "Size distribution of sea salt emissions as a function of relative humidity". *Atmos. Environ.* 40, 588–590. <http://dx.doi.org/10.1016/j.atmosenv.2005.08.043>.
- Markakis, K., Poupkou, A., Melas, D., Tzoumaka, P., Petrakakis, M., 2010. A computational approach based on GIS technology for the development of an anthropogenic emission inventory of gaseous pollutants in Greece. *Water Air Soil Pollut.* 207, 157–180.
- Markakis, K., Katragkou, E., Poupkou, A., Melas, D., 2013. MOSESS: a new emission model for the compilation of model-ready emission inventories. Application in a coal mining area in Northern Greece. *Environ. Model. Assess.* 18 (5), 509–521.
- Martensson, E.M., Nilsson, E.D., de Leeuw, G., Cohen, L.H., Hansson, H.C., 2003. Laboratory simulations and parameterization of the primary marine aerosol production. *J. Geophys. Res.* 108 (D9), 4297. <http://dx.doi.org/10.1029/2002JD002263>.
- Marticorena, B., Bergametti, G., 1995. Modelling the atmospheric dust cycle: 1—design of a soil derived dust production scheme. *J. Geophys. Res.* 100, 16415–16430.
- Menut, L., Foret, G., Bergametti, G., 2007. Sensitivity of mineral dust concentrations to the model size distribution accuracy. *J. Geophys. Res.* 112, D10210. <http://dx.doi.org/10.1029/2006JD007766>.
- Monahan, E.C., Spiel, D.E., Davidson, K.L., 1986. A Model of Marine Aerosol Generation via Whitecaps and Wave Disruption. In: Monahan, E.C., MacNiochaill, G. (Eds.), Oceanic Whitecaps. D. Reidel, Norwell, Mass, pp. 167–193.
- Morectte, J.-J., Boucher, O., Jones, L., Salmond, D., Bechtold, P., Beljaars, A., Benedetti, A., Bonet, A., Kaiser, J.W., Razinger, M., Schulz, M., Serrar, S., Simmons, A.J., Sofiev, M., Suttie, M., Tompkins, A.M., Untch, A., 2009. Aerosol analysis and forecast in the European centre for medium-range weather forecasts integrated forecast system: forward modeling. *J. Geophys. Res.* 114, D06206. <http://dx.doi.org/10.1029/2008JD011235>.
- Mueller, J.F., Mao, Q., Mallard, J.W., 2011. Modelling natural emissions in the community multiscale air quality (CMAQ) model – Part 2: modifications for simulating natural emissions. *Atmos. Chem. Phys.* 11, 293–320. <http://dx.doi.org/10.5194/acp-11-293-2011>.
- Muller, J.F., Stavrakou, T., Wallens, S., De Smedt, I., Van Roozendael, M., Pototsnak, M.J., Rinne, J., Munger, B., Goldstein, A., Guenther, A.B., 2008. Global isoprene emissions estimated using MEGAN, ECMWF analyses and a detailed canopy environment model. *Atmos. Chem. Phys.* 8, 1329–1341. <http://dx.doi.org/10.5194/acp-8-1329-2008>.
- NATAIR, 2007. Ing. Rainer Friedrich. Improving and applying methods for the calculation of natural and biogenic emissions and assessment of impacts to the air quality. Publishable final activity report. In: Sixth Framework Programme FP6-2003-ssp-3 – Policy Oriented Research Specific Targeted Research or Innovation Project Contract No. 513699.

- Pey, J., Querol, X., Alastuey, A., Forastiere, F., Stafoggia, M., 2013. African dust outbreaks over the Mediterranean Basin during 2001–2011: PM10 concentrations, phenomenology and trends, and its relation with synoptic and mesoscale meteorology. *Atmos. Chem. Phys.* 13, 1395–1410. [www.atmos-chem-phys.net/13/1395/2013/doi:10.5194/acp-13-1395-2013](http://www.atmos-chem-phys.net/13/1395/2013/).
- Poupkou, A., Giannaros, T., Markakis, K., Kioutsoukis, I., Curci, G., Melas, D., Zerefos, C., 2010. A model for European biogenic volatile organic compound emissions: software development and first validation. *Environ. Model. Softw.* 25, 1845–1856.
- Poupkou, A., Markakis, K., Liora, N., Giannaros, T., Zanis, P., Im, U., Daskalakis, N., Myriokefalitakis, S., Kaiser, J.W., Melas, D., Kanakidou, M., Karacostas, T., Zerefos, C., 2014. A modeling study of the impact of the 2007 Greek forest fires on the gaseous pollutant levels in the Eastern Mediterranean. *Atmos. Res.* 148, 1–17.
- Schaap, M., Manders, A.M.M., Hendriks, E.C.J., Cnossen, J.M., Segers, A.J.S., Denier van der Gon, H.A.C., Jozwicka, M., 2009. Regional Modelling of Particulate Matter for the Netherlands. Technical background report BOP 500099008. Available at: www.pbl.nl/en.
- Seinfeld, J., Pandis, S.N., 2006. *Atmospheric Chemistry and Physics: from Air Pollution to Climate Change*, second ed. A Wiley-Interscience Publication, John Wiley & Sons, INC., ISBN: 978-0-471-72018-8.
- Shao, Y., Lu, H., 2000. A simple expression for wind erosion threshold friction velocity. *J. Geophys. Res.* 105, 22,437–22,443.
- Shinoda, M., Gillies, J.A., Mikami, M., Shao, Y., December 2011. Temperate Grasslands as a Dust Source: Knowledge, Uncertainties, and Challenges, vol. 3(3). Elsevier. *Aeolian Research*, pp. 271–293.
- Simpson, D., Benedictow, A., Berge, H., Bergstrom, R., Emberson, L.D., Fagerli, H., Flechard, C.R., Hayman, C.D., Gauss, M., Jonson, J.E., Jenkin, M.E., Nyiri, A., Richter, C., Semeena, V.S., Tsyro, S., Tuovinen, J.-P., Valdebenito, A., Wind, P., 2012. The EMEP MSC-W chemical transport model – technical description. *Atmos. Chem. Phys.* 12, 7825–7865. www.atmos-chem-phys.net/12/7825/2012/doi:10.5194/acp-12-7825-2012.
- Skamarock, W.C., Klemp, J.B., Dudhia, J., Gill, D.O., Barker, D.M., Duda, M.G., Huang, X.Y., Wang, W., Powers, J.G., 2008. A Description of the Advanced Research WRF Version 3. NCAR Technical Note, NCAR/TN-475+STR, June 2008. Boulder Colorado, USA, 125pp.
- Soares, J., Sofiev, M., Geels, C., Christensen, J.H., Anderson, C., Lagner, J., Tsyro, S., 2015. Impact of Climate Change on the Production and Transport of Sea Salt Aerosol on European Seas. (As to Be Submitted to Atmospheric Chemistry and Physics (ACP)) (Unpublished results, personal communication with Joana Soares).
- Sofiev, M., Soares, J., Prank, M., de Leeuw, G., Kukkonen, J., 2011. A regional-to-global model of emission and transport of sea salt particles in the atmosphere. *J. Geophys. Res.* 116, D21302. <http://dx.doi.org/10.1029/2010D014713>.
- Steinbrecher, R., Smiatek, G., Koble, R., Seufert, G., Theloke, J., Hauff, K., Ciccioli, P., Vautard, R., Curci, G., 2009. Intra- and inter-annual variability of VOC emissions from natural and semi-natural vegetation in Europe and neighbouring countries. *Atmos. Environ.* 43, 1380e1391.
- Tsyro, S., Aas, W.J., Sofiev, M., Berge, H., Spindler, G., 2011. Modelling of sea salt concentrations over Europe: key uncertainties and comparison with observations. *Atmos. Chem. Phys.* 11, 10367–10388. <http://dx.doi.org/10.5194/acp-11-10367-2011>.
- Van Liedekerke, M., Panagos, P., 2006. Soil Texture Map 10 Km X 10 Km (ETRS_LAEA Version) ESDBv2 Raster Archive - a Set of Rasters Derived from the European Soil Database Distribution Version 2, the European Commission and the European Soil Bureau Network. CD-ROM, EUR 19945 EN.
- Vautard, R., Bessagnet, B., Chin, M., Menut, L., 2005. On the contribution of natural aeolian sources to particulate matter concentrations in Europe: testing hypotheses with a modelling approach. *Atmos. Environ.* 39 (18), 3291–3303. <http://dx.doi.org/10.1016/j.atmosenv.2005.01.051>.
- Vogel, H., Pauling, A., Vogel, B., 2008. Numerical simulation of birch pollen dispersion with an operational weather forecast system. *Int. J. Biometeorol.* 52 (8), 805–814.
- Webb, R.W., Rosenzweig, C.E., Levine, E.R., 2000. Global Soil Texture and Derived Water-holding Capacities. Data Set Available On-line from Oak Ridge National Laboratory Distributed Active Archive Center (Oak Ridge, Tennessee, U.S.A.).
- Winiwarter, W., Bauer, H., Caseiro, A., Puxbaum, H., 2009. Quantifying emissions of primary biological aerosol particle mass in Europe. *J. Atmos. Environ.* 43 (2009), 1403–1409.
- Zender, C.S., Bian, H., Newman, D., 2003. Mineral dust entrainment and deposition (DEAD) model: description and 1990s dust climatology. *J. Geophys. Res.* 108 (D14), 4416–4439.
- Zhang, K.M., Knipping, E.M., Wexler, A.S., Bhave, P.V., Tonnesen, G.S., 2005. Size distribution of sea-salt emissions as a function of relative humidity. *Atmos. Environ.* 39, 3373–3379.